

## Conformational Analysis. The Structure and Composition of the Rotational Conformers of 1,2-Dichlorotetramethyldisilane as Studied by Gas Electron Diffraction

KARI KVESETH

Department of Chemistry, University of Oslo, Blindern, Oslo 3, Norway

Gaseous 1,2-dichlorotetramethyldisilane has been studied by electron diffraction. The more stable conformer in the vapour seems to be *gauche*, contributing with 83(11) % at 40 °C. From the calculated partition functions  $\Delta S = S_g - S_a = 1.4 \text{ cal mol}^{-1} \text{ deg}^{-1}$ , which combined with the determined *gauche/anti* ratio gave  $\Delta E = E_g - E_a = -0.6(5) \text{ kcal mol}^{-1}$ . A model with free, or nearly free, internal rotation has been excluded, but due to the complexity of the molecule, a model with comparatively low torsional barriers cannot be rejected. The main structural parameters ( $r_a$  and  $\angle_a$ ) are: Si–Si = 2.338(13), Si–Cl = 2.077(2), Si–C = 1.860(3), C–H = 1.104(9) (Å),  $\angle \text{SiSiCl} = 107.7(6)$ ,  $\angle \text{SiSiC} = 109.8(7)$ ,  $\angle \text{CSiCl} = 106.4(11)$ ,  $\angle \text{SiCH} = 111.0(16)$ ,  $\phi_g = 76.5(25)$  and  $\phi_{Me} = 71(7)^\circ$ .

In analogy with 1,2-disubstituted ethanes, it is reasonable to expect that also 1,2-disubstituted disilanes may exist as a mixture of two conformers, *gauche* and *anti*. Provided the barrier separating the two forms is high enough, these forms would exist as well-defined geometric species in the vapour, while in a low barrier case a molecule undergoing large amplitude motion<sup>1</sup> with comparatively high probability of intermediate positions, would be observed. If the barrier is very small ( $\lesssim RT/10$ ) essentially free internal rotation will be observed.

In recent studies<sup>2–8</sup> of the Si–Si bond strength, an increasing strengthening of the bond with increasing electronegativity of the substituents has been demonstrated. A quantum mechanical calculation<sup>8</sup> indicates that this strengthening originates from increasing *d*-character in the Si–Si  $\sigma$ -bond.

Due to the rather long Si–Si bond, the steric hindrance in disilanes seems in general to be small. There may even be attractive interactions between the substituents at certain torsional positions. The torsional potential in these molecules consequently may be expected to show rather small variations with substitutional changes compared with, for instance, disubstituted ethanes.

The vibrational spectra of hexasubstituted disilanes<sup>4,7,9–14</sup> have been interpreted as belonging either to the  $D_{3h}/D_{3h}$  symmetry group, or to  $D_{3d}$ . The first two symmetry groups correspond to an *eclipsed* and a freely rotating molecule, respectively.  $D_{3d}$ -symmetry, corresponding to a *staggered* model, has been applied more recently,<sup>14</sup> even though no complete mutual exclusion does exist between the observed IR and Raman frequencies (in liquid).

The four disilanes<sup>16–22</sup> previously studied by electron diffraction exhibit low torsional barriers about the Si–Si axis and a favourable *eclipsed* conformation has definitely been ruled out. An *ab initio* calculation<sup>15</sup> on disilane itself gave a barrier equal to 0.55 kcal mol<sup>-1</sup>. The long H...H distances can unfortunately not be determined by electron diffraction.<sup>16</sup> The torsional motion as studied in hexafluoro-<sup>17</sup> and hexachlorodisilane<sup>1,17–21</sup> gave a preference for *staggered* conformation, with a torsional barrier in the *eclipsed* position of 0.5–1.0 kcal mol<sup>-1</sup>. For molecules with these barriers or larger, electron diffraction cannot distinguish between a *staggered* model description or a description based upon integration of geometric species for all torsional angles.<sup>1,20a</sup>

Rather large average deviations from the *staggered* position (expressed by  $\sigma_\phi$ ) was found in

hexafluorodisilane<sup>18</sup> ( $\sigma_\phi = 25.4^\circ$ ) and in hexamethyldisilane<sup>22</sup> ( $\sigma_\phi = 10^\circ$ ). Altogether structural studies indicate a weak steric hindrance of the torsional motion, with a slightly increased barrier with an increasing size of substituents.

In order to study the torsional behaviour about the Si–Si bond further, 1,2-dichlorotetramethyldisilane has been investigated. Based upon the above discussion and upon the support given by spectroscopic data<sup>5,23</sup> and dipol moment measurements,<sup>8,23</sup> it seems reasonable to expect that a conformational mixture exists in the gas phase.

The *gauche/anti* ratio ( $K$ ) may be studied by the gas electron-diffraction method,<sup>24–28</sup> considering  $K$  as one of the structural parameters in addition to the geometric and vibrational ones. Combined with appropriately calculated partition functions,  $Q$ , the thermodynamic data may be determined.

If, on the other hand, the torsional barrier is smaller than  $0.5 \text{ kcal mol}^{-1}$ , the torsional potential may be determined from the electron-diffraction data.<sup>1,29,30</sup> Usually a classical Boltzmann probability distribution is assumed and the torsional potential is expressed by a terminated Fourier expansion series.

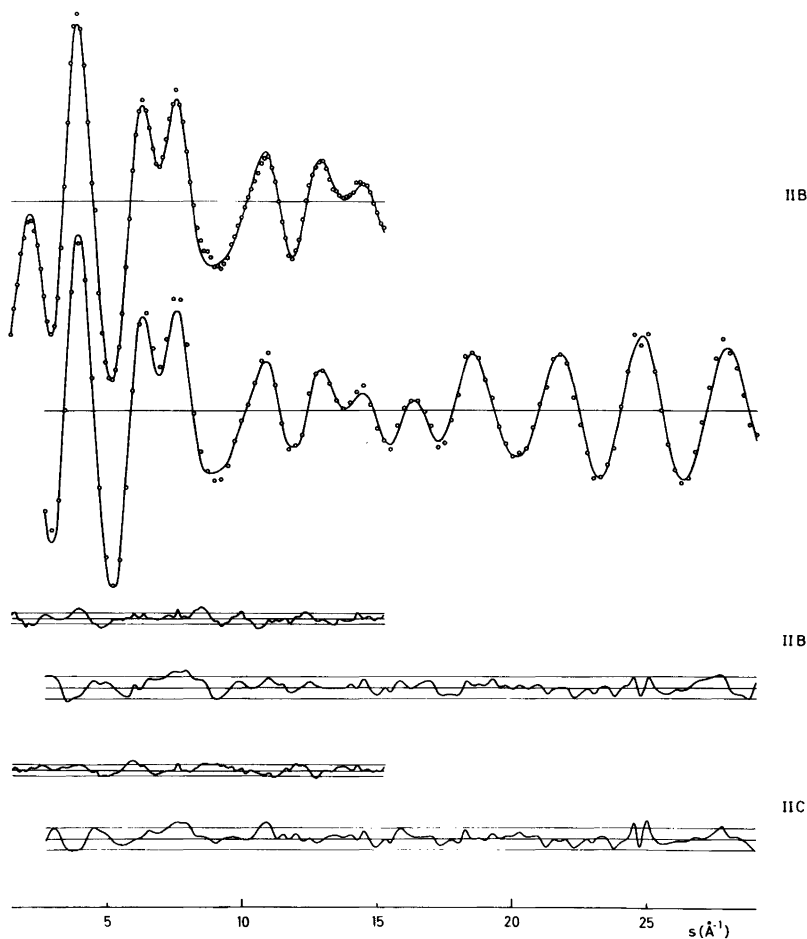


Fig. 1. Intensity curves, 50 cm the upper, 25 cm the lower curve, and difference curves below. The solid curves are theoretical, calculated from the parameters in Table 3, II B. The open circles are experimental values, the difference is experimental minus theoretical, and the lower difference curves are based upon the parameters of Table 3, II C. The limits are  $3\sigma$ ,  $\sigma$  being the experimental standard deviation in the observed points.

## EXPERIMENTAL

The sample of 1,2-dichlorotetramethyldisilane was kindly supplied by Prof. Dr. E. Hengge, Technische Universität, Graz, Austria. Electron-diffraction photographs were obtained with the Balzers Eldigraph KDG-2 unit.<sup>31,32</sup> The experimental conditions were as follows: Nozzle-to-plate distance 500.12 mm (6 plates) and 250.12 mm (6 plates), wavelength, as determined by calibration of ZnO to benzene, 0.058579 Å, nozzle temperature 40 °C. Range of data was 1.000–15.625 and 2.250–30.000 (Å<sup>-1</sup>) with  $\Delta S=0.125$  and 0.250 (Å<sup>-1</sup>), respectively. The optical densities were measured by a Joyce-Loebl MK 111 C densitometer.<sup>27</sup> The data were corrected in the usual way,<sup>33</sup> giving one intensity curve for each photographic plate. The intensities were modified with the function  $s/|f_{Cl}|^2$ .

The computer drawn background<sup>34</sup> was subtracted separately from each intensity curve on levelled form. The averages for each set of plates are presented in Fig. 1.

The relative amount of each conformer, as well as the structural parameters, was determined by conventional least-squares refinement on the combined, but not connected, intensity data.

The theoretical molecular intensities were calculated according to eqn. 11 of Ref. 33. The scattering amplitudes and phase shifts<sup>33,35</sup> were calculated analytically by a program originally written by Yates,<sup>36</sup> using Hartree-Fock-Slater potentials<sup>35</sup> for C, Si and Cl, and a molecular bonded potential for H.<sup>37</sup>

## STRUCTURE ANALYSIS AND REFINEMENT

Radial distribution curves (RD-curves), calculated from the molecular intensities by a Fourier transformation,<sup>33</sup> are presented in Fig. 2. The bond distances, as well as  $r(H_4 \cdots H_4)$  and  $r(Si_1 \cdots H_4)$  contribute to the first four peaks, the  $r(C-H)$  peak being the only completely isolated one. The peak

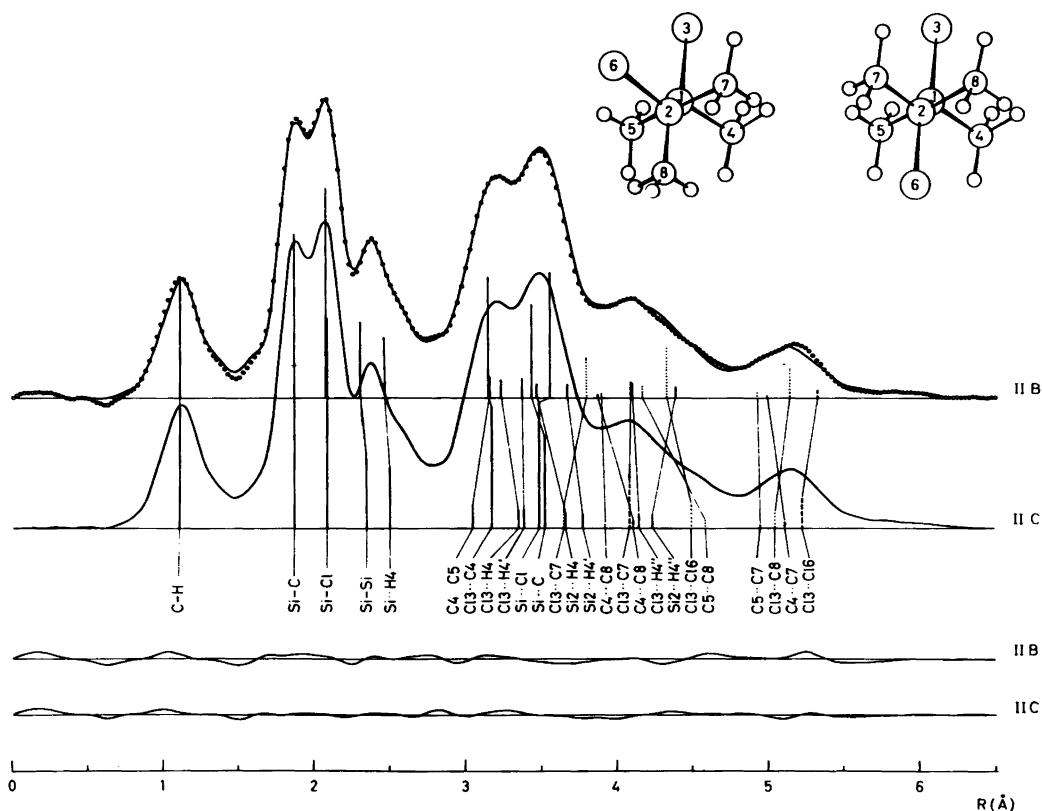


Fig. 2. Radial distribution curves and differences (below) ( $B=0.0025 \text{ \AA}^2$ ). Curve II B corresponds to that column in Table 3, curve II C correspondingly.

complex between 3.0 and 3.7 Å corresponds mainly to non-bonded distances over one angle ( $r(\text{Cl}_3 \cdots \text{C}_4)$ ,  $r(\text{C}_4 \cdots \text{C}_5)$ ,  $r(\text{Si} \cdots \text{C})$  and  $r(\text{Si} \cdots \text{Cl})$ ). The torsional dependent  $\text{Cl} \cdots \text{Cl}$ ,  $\text{Cl} \cdots \text{C}$  and  $\text{C} \cdots \text{C}$  distances contribute to the peak complex between 3.7 and 5.6 Å, together with several distances involving hydrogen atoms, with low contributions.

The area and shape of this outer peak complex is dependent of the torsional distribution about the Si–Si axis.

The following parameters were chosen as independent structural parameters: The four bond distances,  $r(\text{Si} - \text{Si})$ ,  $r(\text{Si} - \text{Cl})$ ,  $r(\text{Si} - \text{C})$  and  $r(\text{C} - \text{H})$ , the angles  $\angle \text{SiSiCl}$ ,  $\angle \text{SiSiC}$ ,  $\angle \text{SiCH}$ , the projected  $\text{CSiC}$ -angle, PV, the methyl twist angle,  $\phi_{\text{Me}}$ , (all four methyls are twisted clockwise) and the torsional angle about the Si–Si axis,  $\phi$ .  $\phi$  is defined as 180° in *anti*, PV is equal to 120° if there is angular  $\text{C}_3$  symmetry in the  $\text{SiClC}_2$ -groups and  $\phi_{\text{Me}} = 60^\circ$  when the methyl groups are *staggered*.

To compensate for the shrinkage effect<sup>38,39</sup> the molecular structure was calculated in the geometric consistent  $r_\alpha$ -picture.<sup>40</sup> The bond distances were transformed to  $r_\alpha$  before calculating the dependent distances by the eqn.  $r_\alpha = r_a + u^2/r - k = r_a + D$ .  $u$  is the root-mean-square vibrational amplitude,  $k$  the perpendicular amplitude correction coefficient,<sup>40,41</sup> and  $r_a$  the operative electron diffraction parameter.

The Si–Si torsional independent parameters of the molecules were assumed to be identical for all values of  $\phi$ . The conformational composition in the vapour is thus determined primarily from the torsional dependent  $r(\text{Cl} \cdots \text{Cl})$ ,  $r(\text{Cl} \cdots \text{C})$ ,  $r(\text{C} \cdots \text{C})$ , since the distances involving hydrogen atoms (a) have generally a fairly low contribution to the total scattered intensities, and (b) are not so sensitive to torsional changes about the Si–Si axis. This torsion makes some of these distances longer and others shorter in a complex and smeared out pattern.

A normal coordinate analysis has been carried out to determine a force field (Table 1) in agreement with the observed frequencies.<sup>5</sup> Due to the limited spectroscopic information available, a valence force field (without any coupling terms) has been applied. Particularly the force constants  $f_{\text{SiCl}}$  and  $f_{\text{SiC}}$  are influenced by this simplification, as they both depend on the coupling terms introduced, particularly the bending force constant couplings. (Hengge *et al.*<sup>3-5</sup> give 2.9 mdyn/Å for both.) Usually the calculated  $u$ -values do not change significantly with reasonable shifts in the force fields while the  $D$ -values generally are somewhat more sensitive.

Table 1. Valence force constants.

Stretch (mdyn Å <sup>-1</sup> )	Bend (mdyn Å rad <sup>-2</sup> )
$f_{\text{Si-Si}}$ 1.82	$f_{\text{SiSiCl}}$ 0.66
$f_{\text{Si-Cl}}$ 1.97	$f_{\text{SiSiC}}$ 0.59
$f_{\text{Si-C}}$ 3.01	$f_{\text{ClSiC}}$ 0.44
$f_{\text{C-H}}$ 4.85	$f_{\text{CSiC}}$ 0.84
	$f_{\text{SiCH}}$ 0.43
	$f_{\text{HCH}}$ 0.50
Torsion (mdyn Å rad <sup>-2</sup> )	
$f_{\tau, \text{SiSi}}$ 0.18	
$f_{\tau, \text{SiC}}$ 0.063	

Table 2. The differences,  $D = u^2/r - k$ , between  $r_\alpha$  and  $r_a$  and the vibrational amplitudes,  $u$ , as calculated from the valence force field at 40 °C.

Distance type <sup>a</sup>	$r(\text{Å})$	$D(\text{Å})$	$u(\text{Å})$
Si–Si	2.33	–0.0010	0.056
Si–Cl	2.08	–0.0096	0.054
Si–C	1.86	–0.0115	0.052
C–H	1.10	–0.0495	0.078
Si⋯Cl	3.57	–0.0007	0.112
Si⋯C	3.42	–0.0035	0.113
Cl <sub>3</sub> ⋯C <sub>4</sub>	3.14	–0.0115	0.113
C <sub>4</sub> ⋯C <sub>5</sub>	3.20	–0.0140	0.094
Si <sub>1</sub> ⋯H <sub>4</sub>	2.47	–0.0300	0.123
H <sub>4</sub> ⋯H <sub>4'</sub>	1.78	–0.0772	0.129
Cl <sub>3</sub> ⋯H <sub>4</sub>	3.31	–0.0122	0.232
Cl <sub>3</sub> ⋯H <sub>4'</sub>	4.13	–0.0267	0.131
Si <sub>2</sub> ⋯H <sub>4</sub>	3.56	–0.0058	0.240
Si <sub>2</sub> ⋯H <sub>4'</sub>	4.41	–0.0171	0.130
C <sub>4</sub> ⋯H <sub>5</sub>	3.45	–0.0167	0.213
C <sub>4</sub> ⋯H <sub>5'</sub>	4.11	–0.0309	0.122
(Cl <sub>3</sub> ⋯Cl <sub>6</sub> ) <sub>a</sub>	5.36	0.0014	0.115
(Cl <sub>3</sub> ⋯C <sub>7</sub> ) <sub>a,g</sub>	4.12	0.0028	0.217
(C <sub>4</sub> ⋯C <sub>8</sub> ) <sub>a,g</sub>	3.83	0.0017	0.208
(C <sub>4</sub> ⋯C <sub>7</sub> ) <sub>a,a</sub>	4.99	–0.0008	0.117
(Cl <sub>3</sub> ⋯Cl <sub>6</sub> ) <sub>g</sub>	4.33	0.0066	0.222
(Cl <sub>3</sub> ⋯C <sub>7</sub> ) <sub>g,g</sub>	3.83	0.0039	0.215
(Cl <sub>3</sub> ⋯C <sub>8</sub> ) <sub>g,a</sub>	5.17	0.0001	0.116
(C <sub>4</sub> ⋯C <sub>8</sub> ) <sub>g,g</sub>	3.93	–0.0013	0.211
(C <sub>5</sub> ⋯C <sub>8</sub> ) <sub>g,g</sub>	4.12	0.0001	0.211
(C <sub>5</sub> ⋯C <sub>7</sub> ) <sub>g,a</sub>	4.94	–0.0015	0.117
all Cl⋯H	(3.66–6.00)		0.153–0.358
all C⋯H	(3.41–5.79)		0.153–0.350
all H⋯H	(2.84–6.76)		0.168–0.440

<sup>a</sup> For numbering of atoms see Fig. 2. Suffix a refers to *anti*, g to *gauche*. In the double suffix, the second gives the type of distance considered.

Due to the limited spectroscopic information particularly about the torsional and skeleton deformation modes, all calculated  $u$ -values of torsional dependent *gauche* fragments and over one angle are somewhat more uncertain in the present case than usual.

The calculated<sup>41,42</sup>  $D$ - and  $u$ -values are given in Table 2. The obtained  $u$ -values are quite reasonable compared with those determined for similar molecules.<sup>17,19,43</sup> The vibrational amplitudes that did not refine were given the calculated values.

The  $D$ -values are particularly sensitive to changes in the torsional force constants. The Si-Si torsional frequency ( $\nu_{\tau, \text{SiSi}}$ ) has been assigned to a  $56 \text{ cm}^{-1}$  Raman ( $\beta$ )line. This frequency roughly corresponds

to a barrier in the order of  $6 \text{ kcal mol}^{-1}$ , and agrees obviously with individual conformers in the vapour. A barrier more in accordance with the experimental findings in the hexasubstituted disilanes would require that  $\nu_{\tau, \text{SiSi}}$  should be closer to  $20 \text{ cm}^{-1}$ . However, an attempt at determining this torsional force constant ( $f_{\tau, \text{SiSi}}$ ) from the torsional dependent  $u$ -values (*i.e.* all *gauche* fragments refined in a group, Table 3,C) indicated even a higher barrier.

The Si-C torsional frequencies are unobserved. The corresponding force constant ( $f_{\tau, \text{SiC}}$ ) has been estimated from the torsional barrier in  $\text{SiH}_3-\text{CH}_3$ <sup>44</sup> ( $V_3 = 1.6 \text{ kcal mol}^{-1}$  (MW)), and corresponds to a torsional frequency at  $180 \text{ cm}^{-1}$ .

Even considering these uncertainties, the esti-

Table 3. Molecular parameters, distances ( $r_a$ ) and vibrational amplitudes ( $u$ ) in Å, angles ( $\angle_a$ ) in degrees. Standard deviations ( $\sigma$ ) in parantheses.  $R_2 = (\sum w\Delta^2 / \sum wI^2)^{1/2} \times 100$ ,  $R_3 = (\text{VPV}/\text{IPI})^{1/2} \times 100$ .<sup>45,46</sup> The shrinkage effects are included in II. Only geometric parameters are refined in A, the  $u$ -values over one angle are refined in one group in B, and individually in C.

	I			II		
	A	B	C	A	B	C
$r(\text{Si}-\text{Si})$	2.342(6)	2.330(14)	2.346(8)	2.341(6)	2.338(13)	2.347(8)
$r(\text{Si}-\text{Cl})$	2.078(2)	2.075(2)	2.080(2)	2.078(2)	2.077(2)	2.080(2)
$r(\text{Si}-\text{C})$	1.859(7)	1.860(3)	1.860(3)	1.860(2)	1.860(3)	1.860(3)
$r(\text{C}-\text{H})$	1.104(9)	1.102(9)	1.101(8)	1.106(9)	1.104(9)	1.104(9)
$\angle \text{SiSiCl}$	106.8(4)	107.9(6)	103.7(6)	107.3(4)	107.7(6)	104.1(7)
$\angle \text{SiSiC}$	109.7(5)	109.7(7)	112.7(7)	109.8(5)	109.8(7)	113.5(6)
VP	131.0(20)	130.0(27)	131.9(17)	130.0(24)	129.2(33)	126.7(10)
$\angle \text{SiCH}$	110.0(11)	109.4(15)	112.9(13)	112.0(11)	111.0(16)	113.6(15)
$\angle \text{CSiCl}^a$	106.0(7)	106.0(10)	105.9(5)	106.2(9)	106.4(11)	107.5(4)
$\angle \text{CSiC}^a$	117.9(20)	117.2(28)	114.8(18)	117.0(23)	116.4(32)	110.1(9)
$\angle \text{HCH}^a$	107.9(12)	109.6(15)	105.9(15)	106.8(12)	107.9(16)	105.0(17)
$\phi_g$	75.8(21)	74.0(19)	94.9(27)	76.8(20)	76.5(25)	96.7(35)
$\phi_{\text{Me}}$	60. —	60. — (-)	60. (-)	72.6(55)	71.0(74)	67.3(98)
$u(\text{Si}-\text{Si})$	0.057 —	0.081(12)	0.061(8)	0.057. —	0.075(10)	0.063(8)
$u(\text{Si}-\text{Cl})$	0.047 —	0.044(3)	0.049(3)	0.047 —	0.045(3)	0.048(3)
$u(\text{Si}-\text{C})$	0.045 —	0.040(4)	0.046(4)	0.045 —	0.042(4)	0.046(4)
$u(\text{Si}\cdots\text{Cl})$	0.112 —	0.106	0.171(30)	0.112 —	0.108	0.128(24)
$u(\text{Si}\cdots\text{C})$	0.113 —	0.107	0.103(14)	0.113 —	0.109	0.127(32)
$u(\text{Cl}_3\cdots\text{C}_4)$	0.113 —	0.107 (7) <sup>b</sup>	0.102(14)	0.113 —	0.109 (5) <sup>b</sup>	0.089(8)
$u(\text{C}_4\cdots\text{C}_5)$	0.094 —	0.088	0.125(119)	0.094 —	0.090	0.045(22)
$u(\text{Si}_1\cdots\text{H}_4)$	0.126 —	0.119(22)	0.127(20)	0.126 —	0.126(22)	0.130(19)
$u(\text{Cl}_3\cdots\text{Cl}_6)_g$	0.222 —	0.222(-)	0.173(27) <sup>c</sup>	0.222 —	0.222(-)	0.189(29) <sup>c</sup>
$n_a(\%)$	13.3(71)	7.4(10)	57.2(54)	16.1(75)	16.8(108)	58.7(63)
$R_2(\%)$	8.65	8.11	7.08	8.64	8.14	7.03
$R_3(\%)$	20.56	20.35	19.37	20.53	20.30	19.36

<sup>a</sup> Dependent angles. <sup>b</sup> Refined in a group. <sup>c</sup> All Si-Si torsion dependent *gauche* fragments refined in a group.

Table 4. Correlation coefficients ( $\rho$ ) larger than 0.5 as estimated from refinements II.

	A	B	C
$r(\text{Si}-\text{Si}), \angle \text{SiSiCl}$	-0.58	-0.81	
$r(\text{Si}-\text{Si}), u(\text{Si}_1 \cdots \text{H}_4)$		0.78	0.69
$r(\text{Si}-\text{Cl}), u(\text{Si}-\text{C})$		0.51	
$\angle \text{SiSiCl}, \angle \text{SiSiC}$			-0.67
$\angle \text{SiSiCl}, u(\text{Si}_1 \cdots \text{H}_4)$		-0.60	
$\angle \text{SiSiCl}, \text{PV}$			-0.58
$\angle \text{SiSiC}, u(\text{Si} \cdots \text{Cl})$		0.52	
$\angle \text{SiSiC}, \text{PV}$	-0.73	-0.81	
$\text{PV}, u(\text{C}_4 \cdots \text{C}_5)$			0.53
$\text{PV}, u(\text{Cl}_3 \cdots \text{C}_4)$			0.54
$\angle \text{SiCH}, u(\text{Si}-\text{Si})$		-0.61	
$\phi_g, u(\text{Cl}_3 \cdots \text{Cl}_6)_g$			-0.52
$\phi_g, n_a$		-0.69	-0.70
$n_a, u(\text{Cl}_3 \cdots \text{Cl}_6)_g$			0.67
$u(\text{Si}-\text{Cl}), \gamma_2$		0.50	0.57
$u(\text{Cl}_3-\text{C}_4), u(\text{C}_4 \cdots \text{C}_5)$			0.64
$u(\text{Cl}_3 \cdots \text{C}_4), u(\text{Si}_1 \cdots \text{Cl}_3)$			0.54
$u(\text{Si}_1 \cdots \text{Cl}_3), u(\text{Si}_1 \cdots \text{C}_4)$			-0.94

mated shrinkage corrections improved the least-squares fit. These refinements are presented as final results (Table 3, II). The inclusion of shrinkage affected the obtained conformational ratio to some extent, and it was felt appropriate also to present the results obtained without shrinkage corrections (Table 3, I).

Non-diagonal elements were included in the weight matrix<sup>45,46</sup> in the least-squares refinements. The obtained standard deviations (1  $\sigma$ ), including the uncertainty of 0.1 % in the wavelength, are given in parentheses. The estimated correlation coefficients ( $\rho$ ) larger than 0.5 are given in Table 4.

## RESULTS AND DISCUSSION

The results of two refinements are presented in Table 3. Keeping the differences between  $u(\text{Si} \cdots \text{Cl})$ ,  $u(\text{Si} \cdots \text{C})$ ,  $u(\text{Cl}_3 \cdots \text{C}_4)$  and  $u(\text{C}_4 \cdots \text{C}_5)$  constant as calculated from the force field, the conformational ratio refined to a predominance of *gauche* (83.2(108) %, Table 3, II B). If, on the other hand, these four  $u$ -values are refined independently, a better fit is obtained, and a predominance of *anti* is found (58.7(63) %, Table 3, II C).

The obtained distance parameters are not significantly different in the two approaches and will be discussed firstly. The Si-Si distances reported in literature varies from 2.24 Å<sup>20</sup> to 2.342 Å.<sup>47</sup> The

Si-Si distance obtained in  $\text{Si}_2\text{Cl}_2(\text{CH}_3)_4$  is in good agreement with the same distance in  $\text{Si}_2(\text{CH}_3)_6$ <sup>22</sup> (2.340(9) Å) and in disilane<sup>16</sup> (2.332(3) Å), but is somewhat larger than reported for  $\text{Si}_2\text{F}_6$ <sup>17</sup> (2.317(6) Å) and the later data for  $\text{Si}_2\text{Cl}_6$ <sup>21</sup> (2.324(30) Å), and definitely larger than the earlier reported values.<sup>19,20</sup>

$r(\text{Si}-\text{C})$  is slightly shorter than that previously reported (1.877(2) Å in  $\text{Si}_2(\text{CH}_3)_6$ <sup>22</sup> and 1.868(2) Å in  $(\text{CH}_3)_3\text{SiH}$ <sup>48</sup>).  $r(\text{Si}-\text{Cl})$  is appreciably longer than found in related compounds (2.009(4)–2.02(2) Å in  $\text{Si}_2\text{Cl}_6$ <sup>19-21</sup> and 2.01(1) Å in  $\text{SiCl}_3\text{CCl}_3$ <sup>19</sup>). On the other hand, such long Si-Cl distances have been found in  $\text{SiCl}_3\text{CH}=\text{CH}_2$ <sup>49</sup> (2.060(5) Å),  $\text{Ph}-\text{SiH}_2\text{Cl}$ <sup>50</sup> (2.076(10) Å) and in  $\text{Ph}-\text{SiCl}_3$ <sup>51</sup> (2.040(10) Å).

Due to the low resolution between  $r(\text{Si}-\text{Cl})$  and  $r(\text{Si}-\text{Si})$ , the refined values of these distances are strongly correlated with the corresponding  $u$ -values. The different values of these distances, as well as the split between them, obtained in the case of  $\text{Si}_2\text{Cl}_6$ , are primarily reflecting the differences in the applied  $u$ -values.<sup>19-21</sup> The Si-Si distance is the most uncertain, as the dominant Si-Cl contribution is almost covering the Si-Si peak. However, keeping the  $u$ -values for all bond distances as well as for the  $\text{Si}_1 \cdots \text{H}_4$  distances equal to the calculated values in this investigation, did not change any of the geometrical parameters significantly (Table 3, A and B).

The obtained bond distances in this molecule are in general good agreement with the observations earlier referred to as the interrelation between the strengthening of bonds from Si-atoms and the electronegativity of substituents.<sup>2-8</sup>

The obtained bond angles as given in column B seem to agree generally better with results from related compounds than those of column C. However, the unsymmetrically substituted Si-groups make such comparisons somewhat questionable. ( $\text{Si}_2\text{Cl}_6$ :<sup>21</sup>  $\angle \text{SiSiCl} = 109.5(10)^\circ$ ,  $\text{Si}_2(\text{CH}_3)_6$ :<sup>22</sup>  $\angle \text{SiSiC} = 108.4(4)^\circ$   $\angle \text{SiCH} = 108.7(8)^\circ$ ,  $\text{Si}_2\text{F}_6$ :<sup>17</sup>  $\angle \text{SiSiF} = 110.3(3)^\circ$ ). Compared with other molecules ( $\text{SiCl}_3\text{CCl}_3$ :<sup>19</sup>  $\angle \text{CSiCl} = 108. (1)^\circ$ ,  $(\text{CH}_3)_3\text{SiCl}$ <sup>52</sup> (MW):  $\angle \text{CSiCl} = 110.5(20)^\circ$ ,  $\text{CH}_3\text{SiCl}_3$ <sup>53</sup> (MW):  $\angle \text{CSiCl} = 109.5^\circ$ ,  $(\text{CH}_3)_3\text{SiH}$ :<sup>48</sup>  $\angle \text{CSiC} = 111.2(2)^\circ$ ) it is demonstrated that a preference of model type B over C is mainly based upon the reported torsional barriers in disilanes, which are compatible with a *staggered* molecular model and, therefore, disagree with the torsional angle of  $96.7(35)^\circ$  obtained in refinement C.

The study of the  $u$ -values does not contribute to

elucidating the problem of conformational preference, due to the uncertainties in the calculated values. When refined in a group (B) or individually (C), the resulting  $u$ -values are reasonable, an exception being  $u(C_4 \cdots C_5)$  which has obtained an unreasonable small value in column C. Keeping  $u(C_4 \cdots C_5)$  at the calculated value did not affect the result, due to the fairly low contribution from this distance.

It is also relevant at this point to emphasize that the obtained conformational ratio is almost independent of whether the torsional dependent  $u$ -values are refined or kept constant. The differences in  $\phi_g$  and  $n_a$  obtained in refinements B and C therefore do not reflect that these  $u$ -values have been refined in one group in refinement C.

The two key parameters describing the conformational relations, the *gauche* torsional angle and the

conformational ratio, seem primarily to be correlated to the differences in the  $u$ -values of the distances over one angle. Including individual  $u$ -values in the refinement leads primarily to changes in the bond angles, and consequently to changes in the conformational parameters. This is demonstrated by the line diagrams in Fig. 2.

In order to elucidate in some detail the information obtainable about the torsional properties, and thereby be able to evaluate the two different results from the refinements, the outer, torsional dependent RD-curves for several theoretical models are presented in Figs. 3 and 4. In Fig. 3 are given the curves for 100% *gauche* (D) and 100% *anti* (E), based upon the structural parameters given in Table 3, II B, together with the theoretical curve obtained in the refinement.

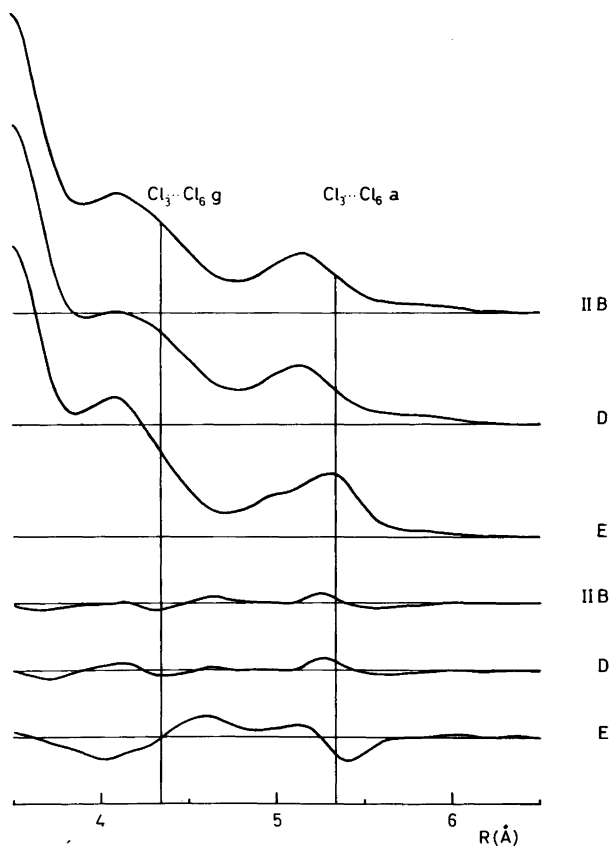


Fig. 3. Radial distribution curves and differences (below) ( $B=0.0025 \text{ \AA}^2$ ). The outer part corresponds to the parameters in Table 3, II B and D, 100% *gauche*; E, 100% *anti*. The differences are experimental minus theoretical curves.

In Fig. 4 are given theoretical curves based upon the structural parameters in Table 3, II C. Curve II C is the outer theoretical curve for that set of parameters, whereas curves F–H correspond to low barrier cases described by a Boltzmann distribution in a three term Fourier expanded potential ( $V(\phi) = \frac{1}{2} \sum_{n=1}^3 V_n(1 + \cos n\phi)$ ). The restricted rotation has a preference for *gauche* in F,  $\Delta E = E_g - E_a = -0.6$  kcal mol<sup>-1</sup> (*vide infra*), and for *anti* in G,  $\Delta E = 0.8$  kcal mol<sup>-1</sup>. The barriers were assumed to be about

1 kcal mol<sup>-1</sup> above the highest minimum. Curve H corresponds to free internal rotation. The *u*-framework values applied have been taken from the estimates of  $u(\text{Cl}\cdots\text{Cl})^{\text{fr}}$  in  $\text{Si}_2\text{Cl}_6$ ,<sup>19</sup> and the same function scaled to  $u(\text{Cl}\cdots\text{C})_a$  and  $u(\text{C}\cdots\text{C})_a$  has been used for  $u(\text{Cl}\cdots\text{C})^{\text{fr}}$  and  $u(\text{C}\cdots\text{C})^{\text{fr}}$ , respectively.

From the curves of Figs. 3 and 4 it is obvious that the structural parameters obtained in refinement II B (Table 3) are consistent with a major proportion of the molecules in *gauche*, and that a model with two isolated species is in satisfactory

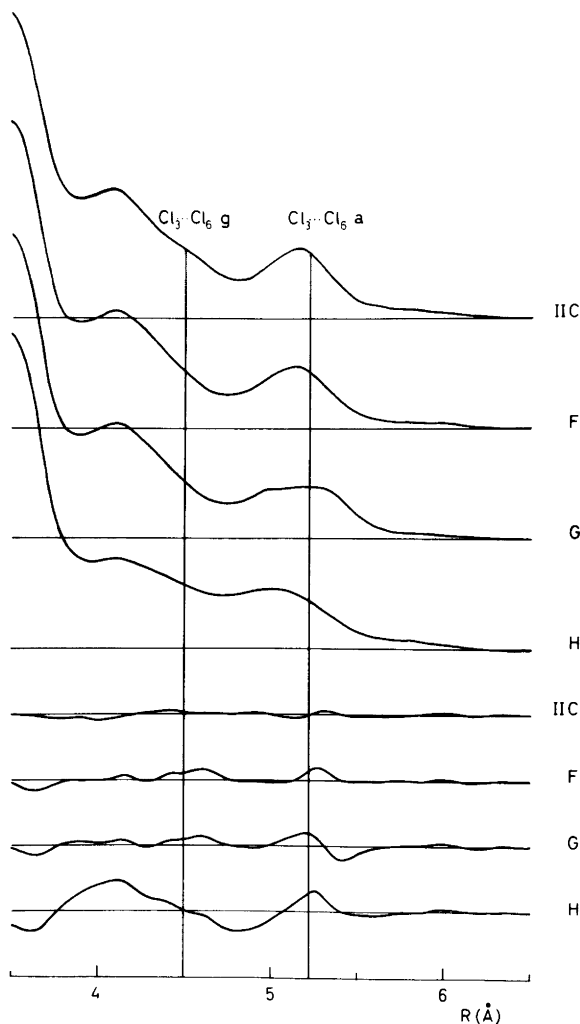


Fig. 4. Radial distribution curves and differences (below) ( $B=0.0025 \text{ \AA}^2$ ). The outer part corresponds to the parameters in Table 3, II C and an integrated model in a potential with F, preference for *gauche*; G, preference for *anti*; and H, with free internal rotation. The differences are experimental minus theoretical curves.



Table 5. Thermodynamic data obtained from estimated mol fraction ( $K=n_g/n_a$ ) and partition functions ( $Q$ ), calculated from the valence force field ( $\nu_{\tau,g}=52\text{ cm}^{-1}$  and  $\nu_{\tau,a}=52\text{ cm}^{-1}$ ) and the principal moments of inertia [ $(I_A I_B I_C)_g=2.393443 \times 10^8\text{ (amu}\cdot\text{\AA}^2)^3$  and  $(I_A I_B I_C)_a=2.469441 \times 10^8\text{ (amu}\cdot\text{\AA}^2)^3$ ].

$R \ln(Q_g/Q_a)$	$-0.010\text{ cal mol}^{-1}\text{ deg}^{-1}$
$RT \partial/\partial T \ln(Q_g/Q_a)$	$-0.002\text{ cal mol}^{-1}\text{ deg}^{-1}$
$\Delta E$	$-0.57\text{ kcal mol}^{-1}$
$\Delta S$	$1.37\text{ cal mol}^{-1}\text{ deg}^{-1}$

agreement with the observations. Based upon the usual formulas<sup>24,25,54</sup> the conformational energy difference,  $\Delta E=E_g-E_a$ , has been determined from the given *gauche/anti* ratio combined with the appropriate vibrational/rotational partition functions ( $Q$ ).  $Q$  has been calculated from the valence force field and the products of the principal moments of inertia. The results are presented in Table 5.

The estimated partition functions are rather uncertain, and in particular influenced by shifts in the torsional frequencies of the two conformers. As  $\Delta S$  differs very little from  $R \ln 2$  (2 being the statistical weight of *gauche*) any reasonable differences in the torsional force constants of the two conformers will have only minor effects on the  $Q_g/Q_a$  ratio and the obtained energy difference.

The obtained  $\Delta E$  value is large compared with previously determined barriers in hexasubstituted disilanes, and opposite in sign to that determined from dipole moment measurements of the liquid.<sup>8</sup> The *gauche* preference is reasonable since the Cl...Cl *gauche* distance corresponds perfectly with the minimum in the Cl...Cl potential, as estimated by molecular mechanics calculations.<sup>55</sup>

Although the results presented in column B (Table 3) seem very probable, a final conclusion about the torsional properties based on this rigid model approach is not straightforward. Inspection of the theoretical curves in Fig. 4 gives a basis to understanding the results obtained in refinement C. This result can, therefore, not be rejected, although the torsional angle of  $96.7^\circ$  certainly seems unreasonable.

Based upon the theoretical curves of Fig. 4 a freely rotating molecule can definitely be ruled out (H). However, the satisfactory fit of both the integrated low barrier models (F and G) illustrates that the unexpected torsional *gauche* angle obtained

in refinement C must be understood as a least-squares fit of an inadequate model. The large torsional angle is not physically real. It reflects that on average more molecules will have geometries in between *gauche* and *anti* than is possible to describe by the usual harmonic approximation at the minima of the torsional potential. The lesson to be learned from this is that an apparent conformational mixture, with an unreasonably large torsional angle, strongly indicates that the torsional potential actually is very wide, and that a more flexible model approach should be introduced.

The second surprising feature observed when the low barrier model is introduced is the apparent *anti* preference obtained in the inadequate model description. Although the applied potentials have been estimated rather roughly, the better fit of curve F indicates that even refinement C is compatible with *gauche* as the more favourable conformer.

Based on the electron-diffraction data alone we cannot discriminate between the two obtained molecular models. The calculated  $u$ -values from spectroscopic data, as well as the experience obtained from studies on related compounds, seem to support model B, giving two isolated geometric species with a *gauche* preference in the vapour. But as the refined  $u$ -values in refinement C are not unreasonable, a model with fairly low torsional barriers cannot be rejected. Also in that case the potential minimum close to  $60^\circ$  (the *gauche* position) probably has the lower value.

The temperature applied in these calculations is measured at the nozzle tip by a thermocouple. Previous experience has justified that within the present level of accuracy the nozzle temperature may be used as the temperature of the gaseous mixture.<sup>1</sup>

*Acknowledgements.* I am indebted to Prof. E. Hengge and his coworkers for suggesting this project and for synthesizing the compound. Siv.ing. R. Seip should also be thanked for recording the electron-diffraction data and Mrs. S. Gundersen for photometering the plates as well as running the first computer programs and drawing the figures. I am also grateful to Prof. O. Bastiansen for his interest in this work and for helpful discussions. Financial support by NAVF is gratefully acknowledged.

## REFERENCES

1. Bastiansen, O., Kveseth, K. and Møllendal, H. *Curr. Chem. Top.* 81 (1979) 99.
2. Hengge, E. *Curr. Chem. Top.* 51 (1974) 1.
3. Höfler, F., Sawodny, W. and Hengge, E. *Spectrochim. Acta A* 26 (1970) 819.
4. Höfler, F., Waldhör, S. and Hengge, E. *Spectrochim. Acta A* 28 (1972) 29.
5. Höfler, F. and Hengge, E. *Monatsh. Chem.* 103 (1972) 1506.
6. Hengge, E. and Waldhör, S. *Monatsh. Chem.* 105 (1974) 671.
7. Höfler, F. *Unpublished results.*
8. Nagy, J., Ferenczi-Gresz, S., Hengge, E. and Waldhör, S. *Kem. Kozl.* 46 (1976) 424.
9. Cerato, C. C., Lauer, J. L. and Beachell, H. C. *J. Chem. Phys.* 22 (1954) 1.
10. Murata, H. and Shimizu, K. *J. Chem. Phys.* 23 (1955) 1968.
11. Bürger, H. and Falnus, H. *Z. Anorg. Allg. Chem.* 363 (1968) 24.
12. Morino, Y. *J. Chem. Phys.* 24 (1956) 164.
13. Katayama, M., Shimanouchi, T., Morino, Y. and Mizushima, S. *J. Chem. Phys.* 18 (1950) 506.
14. Pfeiffer, M. and Spangenberg, H. *J. Z. Phys. Chem.* 232 (1966) 47.
15. Hinchliffe, A. *J. Mol. Struct.* 48 (1978) 279.
16. Beagley, B., Conrad, A. R., Freeman, J. M., Monaghan, J. J., Norton, B. G. and Holywell, G. C. *J. Mol. Struct.* 11 (1972) 371.
17. Oberhammer, H. *J. Mol. Struct.* 31 (1976) 237.
18. Rankin, D. W. H. and Robertson, A. *J. Mol. Struct.* 27 (1975) 438.
19. Morino, Y. and Hirota, E. *J. Chem. Phys.* 28 (1958) 185.
20. a. Swick, D. A. and Karle, J. L. *J. Chem. Phys.* 23 (1955) 1499; b. Karle, J. L. *J. Chem. Phys.* 45 (1966) 4149.
21. Haase, J. *Z. Naturforsch. Teil A* 28 (1973) 542.
22. Beagley, B., Monaghan, J. J. and Hewitt, T. G. *J. Mol. Struct.* 8 (1971) 401.
23. Hayashi, M. *Nippon Kagaku Zasshi* 79 (1958) 775.
24. Kveseth, K. *Acta Chem. Scand. A* 28 (1974) 482.
25. Kveseth, K. *Acta Chem. Scand. A* 29 (1975) 307.
26. Almenningen, A., Fernholt, L. and Kveseth, K. *Acta Chem. Scand. A* 31 (1977) 297.
27. Fernholt, L. and Kveseth, K. *Acta Chem. Scand. A* 32 (1978) 63.
28. Fernholt, L. and Kveseth, K. *Acta Chem. Scand. A* 33 (1979) 335.
29. Almenningen, A., Hartmann, Å. O. and Seip, H. M. *Acta Chem. Scand.* 22 (1968) 1013.
30. Kveseth, K., Seip, H. M. and Stølevik, R. *Acta Chem. Scand.* 25 (1971) 2975.
31. Zeil, W., Haase, J. and Wegmann, L. *Z. Instrumentenk. 74* (1966) 84.
32. Bastiansen, O., Graber, R. and Wegmann, L. *Balzers High Vacuum Report* 25 (1969) 1.
33. Andersen, B., Seip, H. M., Strand, T. G. and Stølevik, R. *Acta Chem. Scand.* 23 (1969) 3224.
34. a. Hedberg, L. *5th Austin Symposium on Gas Phase Molecular Structure* 37 (1974); b. Gundersen, G. and Samdal, S. *The Norwegian Electron-Diffraction Group, Annual Report, NAVF*, 9 (1976).
35. Strand, T. G. and Bonham, R. A. *J. Chem. Phys.* 40 (1964) 1686.
36. Yates, A. C. *Comput. Phys. Commun.* 2 (1971) 175.
37. Stewart, R. F., Davidson, E. R. and Simpson, W. T. *J. Chem. Phys.* 42 (1965) 3175.
38. a. Almenningen, A., Bastiansen, O. and Munthe-Kaas, T. *Acta Chem. Scand.* 10 (1956) 261; b. Almenningen, A., Bastiansen, O. and Trætteberg, M. *Acta Chem. Scand.* 13 (1959) 1699.
39. Morino, Y. *Acta Crystallogr.* 13 (1960) 1107.
40. Kuchitsu, K. *Bull. Chem. Soc. Jpn.* 44 (1971) 96.
41. Stølevik, R., Seip, H. M. and Cyvin, S. *J. Chem. Phys. Lett.* 15 (1972) 263.
42. Gwinn, W. D. *J. Chem. Phys.* 55 (1971) 477.
43. Morino, Y., Kuchitsu, K., Takahashi, A. and Maeda, K. *J. Chem. Phys.* 21 (1953) 1927.
44. Hirota, E. *J. Mol. Spectrosc.* 43 (1972) 36.
45. Seip, H. M., Strand, T. G. and Stølevik, R. *Chem. Phys. Lett.* 3 (1969) 617.
46. Seip, H. M. and Stølevik, R. In Cyvin, S. J., Ed., *Molecular Structure and Vibrations*, Elsevier, Amsterdam 1972.
47. Smith, Z., Seip, H. M., Hengge, E. and Bauer, G. *Acta Chem. Scand. A* 30 (1976) 697.
48. Pierce, L. and Petersen, D. H. *J. Chem. Phys.* 33 (1960) 907.
49. Vilkov, L. V., Mastryukov, V. S. and Skishin, P. A. *Zh. Strukt. Khim.* 5 (1964) 183 (168 Engl.).
50. Vilkov, L. V. and Mastryukov, V. S. *Dokl. Akad. Nauk. SSSR* 162 (1965) 1306 (596 Engl.).
51. Vilkov, L. V., Mastryukov, V. S. and Akishin, P. A. *Zh. Strukt. Khim.* 5 (1964) 906 (834 Engl.).
52. Durig, J. R., Carter, R. O. and Li, Y. S. *J. Mol. Spectrosc.* 44 (1972) 18.
53. Mockler, R., Bailey, J. H. and Gordy, W. *J. Chem. Phys.* 21 (1953) 1710.
54. Glasstone, S. *Theoretical Chemistry*, van Nostrand, New York 1964, p. 396.
55. Abraham, R. J. and Stølevik, R. *Private communication.*

Received February 7, 1979.